Journal of Molecular Liquids 328 (2021) 115478

Contents lists available at ScienceDirect

Journal of Molecular Liquids

journal homepage: www.elsevier.com/locate/molliq

On the effects of head-group volume on the adsorption and aggregation of 1-(*n*-hexadecyl)-3-C_m-imidazolium bromide and chloride surfactants in aqueous solutions

Nicolas Keppeler [a], Paula D. Galgano [a], Soraya da Silva Santos [a], Naved I. Malek [b], Omar A. El Seoud [a,*]

[a] Institute of Chemistry, University of São Paulo, São Paulo, SP 05508-000, Brazil
[b] Applied Chemistry Department, Sardar Vallabhbhai National Institute of Technology, Surat, Gujarat 395 007, India

ARTICLE INFO

Article history:
Received 8 December 2020
Received in revised form 17 January 2021
Accepted 22 January 2021
Available online 30 January 2021

Keywords:
Ionic liquid-based surfactants
Surfactant head-group volume
Adsorption and aggregation parameters
Green synthesis
Polarity of micelle interfacial water
Micelle solubilization

ABSTRACT

The effects of the length of alkyl side chain (C_m) of ionic liquid-based surfactants (ILBSs) on their adsorption at the water/air interface, and aggregation in aqueous solutions were investigated for the series 1-(*n*-hexadecyl)-3-C_m-imidazolium bromides and chlorides, where $C_m = C_1$-C_4 for the bromides, and C_1-C_5 for the chlorides. These physicochemical properties were calculated from surface tension, conductivity, and fluorescence data. It was found that increasing the length of C_m (*i.e.*, volume of the head group) leads to enhancement of surface activity, increase in the area per surfactant molecule at the water/air interface (A_{min}) and the degree of counter-ion dissociation (α_{mic}). Our data also indicated that increasing the volume of the head group results in a decrease of the critical micelle concentration (cmc), Gibb's free energy of adsorption and micellization, and microscopic polarity of interfacial water. In order to delineate the effects of the presence of unsaturation in the HG, we included members that carry C_m = vinyl and allyl in the bromide series. The effect of these groups was found to be similar to removing a methylene group from C_m. The dependence of the solubilization of a lipophilic dye (Sudan IV) and a drug (nitrendipine) on the length of C_m was also studied.

1. Introduction

The unique physicochemical properties (high polarity, chemical and thermal stability, and negligible vapor pressure) of ionic liquids (ILs) led to their widespread use of in different research areas, as well as in the chemical and pharmaceutical industries [1–3]. The molecular structural versatility of ILs means that many useful properties, including polarity, miscibility with molecular solvents, and electrochemical behavior can be tailored to the researcher's need by a judicious choice of the structures of the cations and anions [4–6]. For example, ILs markedly improve the pharmacokinetic and pharmacodynamic properties of drugs, overcoming the limitations in drug delivery of water insoluble, or sparingly soluble drugs [5]. Additionally, enzymatic reactions were successfully carried out in IL based aqueous microemulsions with high conversion rates, high enantioselectivity, and better enzyme stability, and recyclability [7–9].

Ionic liquid-based surfactants (ILBSs) are ILs with colloidal properties due to their long-chain hydrophobic "tails". The favorable characteristics of ILs are carried over to ILBSs. Depending on their molecular structures, ILBSs have higher surface activity and lower critical micelle concentration (cmc) as compared with the structurally related "conventional" surfactants [10–15]. The enhanced surface activity of ILBSs is important because less surfactant is required for the end-use. Therefore, knowledge of the adsorption/aggregation behavior of ILBSs is required to develop their applications.

The useful applications of ILBSs, *e.g.*, in nanotechnology, drug delivery, and decontamination depend on their molecular structures, including the hydrophobic chain (HC) length, charge and size of the head group (HG), and nature of the counter-ion. In nanotechnology, for example, the ease of tailoring the properties of ILBSs through molecular modification turns them into efficient templates to control the average size, porosity and morphology of new nanomaterials [16]. Previously, we studied the effect of the length of the HC on the adsorption and micellization properties in water of imidazole-based ILBSs, namely C_nMeImCl, where n = 10, 12, 14 and 16 [17]. The effect of HG size was not studied for many ILBSs, although this structural variable bears on the packing parameter of the monomers in the micellar aggregates, hence their geometries [18]. Effects of this structural variable was evaluated for conventional surfactants, *e.g.*, alkyltrialkylammonium bromides and chlorides. It was found that the values of the cmcs and aggregation numbers (N_{agg}) decrease as a function of increasing the number of methylene groups in the HG [19–22].

* Corresponding author.
E-mail address: elseoud.usp@gmail.com (O.A. El Seoud).

https://doi.org/10.1016/j.molliq.2021.115478
0167-7322/

The objective of the present work is the synthesis and determination of adsorption/aggregation properties of the imidazole-based ILBSs depicted in Fig. 1. As shown, the hydrophobic tail was fixed as *n*-hexadecyl, whereas the other substituent in the imidazolium ring (R) was varied from methyl to *n*-pentyl; the unsaturated groups vinyl and allyl were also included. Data on the adsorption and aggregation properties in water are available only for the following ILBSs: C_{16}MeImBr [23–25], C_{16}EtImBr [12], C_{16}BuImBr [26], C_{16}VnImBr [12] and C_{16}MeImCl [27–29] (Bu, Et, Me, and Vn refer to n-butyl, ethyl, methyl, and vinyl group, respectively). The colloidal properties of the other six members of this ILBS series were not evaluated, while two of them (C_{16}PrImCl and C_{16}PnImCl) are novel (Pn and Pr refer to n-pentyl and n-propyl group, respectively). Similar dialkyl imidazolium-based ILs have been synthesized and studied [30], showing superior surface activity and lower cmc values as compared to single chain imidazolium counterparts.

We used surface tension and conductivity to probe the surfactant adsorption at the water/air interface and its aggregation in aqueous solution. The quantities calculated include: cmc, surface tension at cmc (γ_{cmc}), surface tension reduction efficiency (by 20 mN m^{-1}; pC_{20}), surface excess concentration at the interface (Γ_{max}), minimum area per molecule at the water/air interface (A_{min}), Gibb's free energy of adsorption (ΔG^0_{ads}) and micellization (ΔG^0_{mic}), degree of counter-ion dissociation (α_{mic}). We used the fluorescence spectra of micelle-solubilized pyrene to calculate the concentration of water in the interfacial region. Additionally, we studied the dissolution of a hydrophobic dye (Sudan IV) and nitrendipine, a drug employed for treatment of hypertension [31], because the association of certain substrates, *e.g.*, cyclodextrins that complex drugs show dependence on the structure of the HG [32].

2. Materials and methods

2.1. Materials

The reagents were purchased from Acros, Sigma-Aldrich, Merck or Synth (São Paulo) and were purified as recommended elsewhere [33]. We purified 1-bromo-*n*-hexadecane and 1-chloro-*n*-hexadecane by repeated fractional distillation in a 50 cm long Vigreux column, under reduced pressure. Satisfactory purity was achieved (> 99.9%) as shown by gas chromatographic analysis. Deionized (Milli-Q) water was used throughout.

2.2. Equipment

We used the following equipment:

Synthesis of the ILBSs: Masterflex model 77,390–00 metering pump and CEM Discover (CEM Co.) microwave (MW) equipment, provided with pressure accessory (for chloride ILBSs).

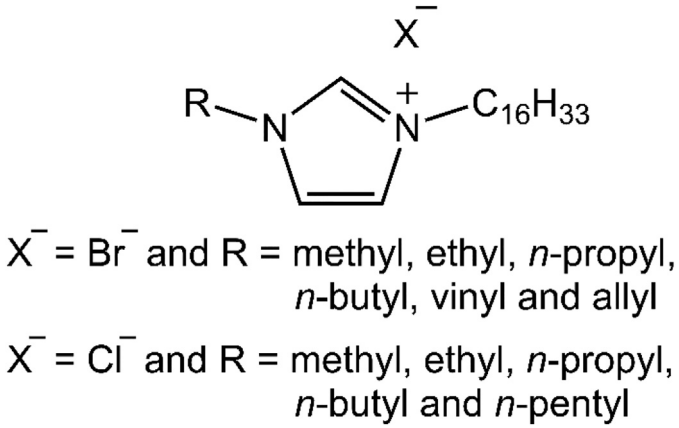

Fig. 1. Molecular structures of the synthesized ILBSs.

Gas chromatography: Shimadzu 17A-2 gas chromatograph, equipped with an FID detector and Supelcowax 10 capillary column.

Melting points: IA 6304 apparatus (Electrothermal), the melting points (m.p.'s) were not corrected.

CHN elemental analyses: Perkin Elmer 2400 CHN apparatus. These analyses were performed in the Analytical Center of this Institute.

^{1}H and ^{13}C NMR spectra: Avance 300 (Bruker), 300 MHz for ^{1}H and 75 MHz for ^{13}C NMR. All samples were dissolved in $CDCl_3$ containing TMS as internal reference.

Conductivity measurement and chloride ion titration: Mettler-Toledo S400 SevenExcellence pH/mV meter with InLab 710 electrode 710 ($K = 0.8\ cm^{-1}$), attached to Lauda E200 thermostat, and Schott Titronic T200 programmed burette.

Solution surface tension: Lauda TVT 2 drop volume tensiometer, attached to Lauda E300 thermostat.

UV–Vis spectra: Shimadzu UV-2550 Spectrophotometer, provided with thermostated cell holder and 4000A digital thermometer (Yellow Springs Instruments).

Fluorescence spectra: Hitachi F-7000 fluorescence spectrophotometer, provided with thermostated cell holder. We used 1 cm path length quartz cuvettes with PTFE stoppers.

2.3. Synthesis of the ILBSs

The ILBSs were synthesized by the reaction schemes shown in Fig. 2. Both series of ILBSs were synthesized *via* microwave-assisted reaction.

2.3.1. 1-Alk(en)ylimidazole

We dissolved sodium metal (0.30 mol) in 100 mL of dry 2-propanol under reflux and magnetic stirring (approx. 2 h). After cooling to room temperature, we added to the reaction flask, under stirring, a solution of imidazole (0.30 mol) in 40 mL of 2-propanol, stirred the mixture for additional 30 min, removed the solvent to yield a yellowish paste, and suspended the latter in 120 mL of dry acetonitrile (MeCN). We put the reaction flask in an ice bath, agitated the suspension vigorously, and used a peristaltic pump to add a solution of 1-bromoalkane or 1-bromoalkene (0.33 mol) in 25 mL of MeCN during 6 h, and then kept the mixture stirred overnight at room temperature. We filtered the precipitated solid, removed the solvent and distilled the product under reduced pressure (~1 mmHg). In all cases we obtained colorless liquids; boiling points at 1 mmHg are 52 °C, 65 °C, 70 °C, 72 °C and 61 °C for 1-R-imidazole, with R = ethyl, *n*-propyl, *n*-butyl, *n*-pentyl, and allyl, respectively. The yields of 1-R-imidazole were from 80 to 90%, based on imidazole. 1-Methylimidazole and 1-vinylimidazole are commercially available.

2.3.2. Bromide ILBSs

We slowly added a solution of 1-bromehexadecane (0.055 mol) in 70 mL of dry ethyl acetate, with efficient stirring to 0.050 mol of the appropriate 1-alk(*en*)ylimidazole and heated the reaction mixture for 5 h at 70 °C in the microwave equipment (60 W irradiation power). We removed the solvent, washed the resulting white solid with *n*-hexane (3 × 25 mL) and dried it under reduced pressure over P_4O_{10} until constant mass. The products were characterized by melting point, ^{1}H NMR, and elemental analysis, vide item 1.1 of Supplementary Material (SM). The ^{1}H NMR spectra of the products are presented in Fig. SM1 to SM6.

2.3.3. Chloride ILBSs

The ILBS C_{16}MeImCl was available from a previous study [17]. We synthesized the other chlorides by reacting 0.050 mol of 1-alkylimidazole with 0.055 mol of 1-chloro-*n*-hexadecane in the pressure reactor (50 mL) of the microwave equipment, under the following conditions: no solvent; irradiation power = 200 W; 170 °C; 20 bar; 5 h. After cooling to room temperature, we washed the product with *n*-hexane (3 × 25 mL) and dried it under reduced pressure over P_4O_{10} until

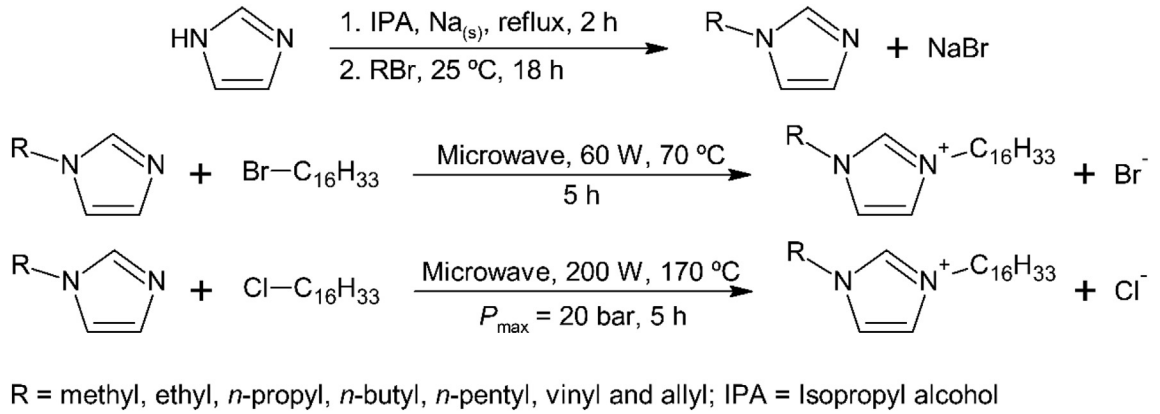

Fig. 2. Reaction schemes for the synthesis of the ILBSs.

constant mass. These surfactants were characterized by their melting point, ^{1}H and ^{13}C NMR, and Volhard titration method for chloride analyses [34]. The results of the analyses are shown in SM and the corresponding ^{1}H and ^{13}C NMR spectra are presented in Fig. SM7-SM14.

2.4. Experimental method

2.4.1. Surface tension measurements

For each surfactant we prepared 12 solutions, whose concentrations were from *ca.* 5 times below the cmc up to 15 times above the cmc. Values of the latter were available from the conductivity measurements, detailed in Section 2.4.2. We recorded the surface tension (γ) of each solution after 10 min temperature equilibration at 25 ± 0.1 °C on the drop volume tensiometer. The outer and inner radius of the steel needle were 1.39 and 1.08 mm, respectively. The measurements of the ILBSs solutions were done with 10 different drop formation velocities (0.5 s mL^{-1} to 5 s mL^{-1}); average = 3 drops at each velocity.

2.4.2. Conductivity measurements

We calibrated the conductivity meter with 0.01 mol L^{-1} KCl aqueous solution. The measurements were made at 25 ± 0.1 °C for all ILBSs, except for C_{16}MeImCl, whose data were published elsewhere [17]. We added 100 μL aliquots of the ILBSs aqueous solutions (*ca.* 5–10 times above cmcs, based on literature values, *e.g.*, of C_{16}MeImBr and C_{16}MeImCl [35,36]) to 10 mL of water, and registered the conductivity after each addition. We used a home-developed software, both for programmed addition of the concentrated surfactant solution to water and acquisition of conductivity data.

2.4.3. Fluorescence measurements

We pipetted 200 μL of 10^{-4} mol L^{-1} methanolic solution of pyrene into 10 mL volumetric flasks, evaporated the solvent, added the appropriate volume of the surfactant solution and water. The final (fixed) concentrations of pyrene and surfactant were 2.0×10^{-6} mol L^{-1} and 10 x cmc, respectively. To ensure complete dissolution of pyrene, we agitated the volumetric flasks overnight (Glas-Col model 099A RD4512 tube rotator; 60 rpm); sonicated the solutions for 15 min (Fritsch, Laborette 17 sonicator) and then waited for another 15 min before recording the spectra at 350–500 nm, using an excitation wavelength of 334 nm, and slit widths of 2.5 nm.

We calculated the effective water concentration as follows: (i) the values of fluorescence intensities ratio of the first and third vibronic peaks (I_1/I_3) for pyrene in the micellar pseudo-phases were calculated; (ii) a calibration curve of I_1/I_3 *versus* [water] in water/1-propanol mixtures, *outside the micellar domain*, was plotted according to literature data [37]; (iii) the I_1/I_3 values (in presence of the ILBS) were converted into interfacial water concentration using the above-mentioned calibration curve. Previous studies showed that water/1-propanol binary mixture is a good model for interfacial water [38].

2.4.4. Dye and drug solubilization

We added an excess of finely powdered Sudan IV or nitrendipine to the surfactant solution (*ca.* 8 x cmc), agitated the suspension for 5 min (vortex mixer) and then overnight using the above-mentioned tube rotator (60 rpm). We removed the undissolved solid by filtration for Sudan IV, using 10 μm PTFE membrane (0.45 μm, 13 mm; Gelman 4422) and centrifugation for nitrendipine (ThermoCientific Sorvall Legend X1R). We diluted the filtrate 5 times with the respective ILBS solution and measured the absorbance of dissolved solubilizate using the above-mentioned Shimadzu spectrophotometer. We recorded the UV–Vis spectra from 440 to 600 nm for Sudan IV and from 300 to 420 nm for nitrendipine solutions at 25.0 ± 0.1 °C and then calculated the concentrations of solubilized dye and drug from the appropriate Beer's law plot.

3. Results and discussion

3.1. General

We synthesized pure chloride ILBSs by a novel, fast, solventless, microwave-assisted route, instead of using literature procedures that require reflux of both reactants in a solvent for 24–48 h [39,40]. This synthesis, besides being greener than its traditional counterparts, gave good yield of pure ILBSs. Use of elemental analysis for assessing the purity of chloride ILBSs was not feasible because of their hygroscopic character, and the waxy, difficult-to-dry nature of the corresponding iodides and perchlorates, therefore we used the Volhard titration method.

For brevity, we use in the discussion below the term HG volume to denote the increase in the length of the side chain attached to the imidazolium ring from methyl- to *n*-pentyl. We use the general structure C_{16}RImX to denote the series studied in the present work, where R refers to the substituent group (saturated and unsaturated) and X refers to Br and Cl. In the first part of each discussion, we consider the results of the saturated groups in the HG, designating them as C_{m}. The effect of presence of unsaturation is discussed subsequently by comparing C_{16}EtImBr with C_{16}VnImBr (2 carbons), and C_{16}PrImBr with C_{16}AlImBr (3 carbons; Al = allyl group).

We discuss the dependence of solution physicochemical properties on the volume of the HG in the following order: adsorption at water/air interface, micelle formation, and concentration of interfacial water. Where appropriate, we compare the effects of increasing HG volume with those caused by increasing the length of hydrophobic chain (C_{n}), *e.g.*, from *n*-decyl to *n*-hexadecyl, keeping the HG structure constant (*i.e.*, C_{10}MeImCl to C_{16}MeImCl [17]). Additionally, some aggregation

properties of the ILBSs series were compared with those of structurally related conventional surfactants. Finally, we discuss the effects of increasing the HG volume on the solubilization of hydrophobic nonionic dye (Sudan IV) and the drug nitrendipine, a dihydropyridine calcium channel-blocker employed in the treatment of primary hypertension [31].

The equations to calculate the parameters of the surfactant adsorption at the water/air interface and aggregation as micelles are standard [18]. Therefore, we show only the results of these calculations; the corresponding equations are presented in supplementary material, SM.

3.2. Adsorption at water/air interface

It is important to measure solution surface tension values after the surfactant adsorption has reached equilibrium; this requires unknown time and can be long for ionic surfactants [41]. Therefore, we measured the surface tension as a function of drop formation time (t), as exemplified in Fig. SM15 for $C_{16}C_m$ImBr. For each surfactant solution, we calculated the surface tension at infinity time (γ_{inf}) by regression analysis of γ *vs.* t. For the studied ILBS series, the difference between the initial surface tension (γ_0) and γ_{inf} reaches 8.5%; this difference affects the calculated adsorption parameters values by up to 20%.

We plot in Fig. 3 the extrapolated values of the surface tension (γ_{inf}) as a function of log [ILBS]. As expected, values of γ_{inf} decrease fast as a function of increasing the surfactant concentration until the cmc, and then decrease much slower. The absence of "dips" in these plots show that the ILBSs are surface active pure [42]. Demonstrating this purity is important, because uncertainty in the cmc value (due to presence of the dip) bears on the calculated adsorption and micellar properties [43,44]; removing surface-active impurities from the solution is, at best, time-consuming and laborious [45].

We employed the surface tension data to calculate the values of cmc and adsorption parameters, including γ_{cmc}, pC_{20}, Γ_{max}, A_{min}, and ΔG^0_{ads}, see Eqs. SM1 to SM4. We present the values of these parameters in Table 1. The cmc values, given by the break in plot of γ_{inf} *versus* log [ILBS], are presented and discussed in Section 3.3.

Where γ_{cmc}, pC_{20}, Γ_{max}, A_{min} and ΔG^0_{ads} stand for surface tension at cmc, surface tension reduction efficiency, surface excess concentration at the interface, minimum area per molecule at the water/air interface and Gibb's free energy of adsorption, respectively.

As seen in Fig. 3, the slopes of the straight lines in the region below the cmc decrease as a function of increasing the HG volume, this corresponds to an increase in the A_{min} and a decrease in Γ_{max}. The increase of

Table 1
Dependence of surfactant adsorption parameters at 25 °C on head group volume of the studied ILBSs.

ILBS	γ_{cmc} (mN m^{-1})	pC_{20}	Γ_{max} (μmol m^{-2})	A_{min} (nm^2)	ΔG^0_{ads} (kJ mol^{-1})
Bromide ILBSs					
C_{16}MeImBr	38.7	3.55	3.0	0.54	−36.83
C_{16}EtImBr	39.8	3.65	2.7	0.61	−38.19
C_{16}PrImBr	39.7	3.80	2.3	0.73	−40.46
C_{16}BuImBr	40.3	3.92	1.9	0.86	−42.73
C_{16}VnImBr	37.7	3.63	3.1	0.53	−37.09
C_{16}AllmBr	38.7	3.74	2.6	0.63	−38.90
Chloride ILBSs					
C_{16}MeImCl	40.9	3.39	3.4	0.49	−35.64
C_{16}EtImCl	35.4	3.62	2.6	0.63	−38.29
C_{16}PrImCl	35.2	3.82	2.2	0.75	−40.78
C_{16}BuImCl	38.0	3.89	2.1	0.80	−41.86
C_{16}PnImCl	39.6	4.15	1.6	1.06	−46.37

A_{min} with C_m is clearly shown in Eqs. (1) and (2) for the $C_{16}C_m$ImX (X = Br and Cl) series, whereas Eq. (3) shows the effect of increasing C_n of the C_nMeImCl series [17]. Eqs. (1), (2) and (3) are linear regressions of the lines in Fig. SM16.

$$C_{16}C_mImBr: A_{min}/nm^2 = 0.42\ (\pm 0.03) + 0.108\ (\pm 0.010)\ C_m, R^2 = 0.975 \quad (1)$$

$$C_{16}C_mImCl: A_{min}/nm^2 = 0.35\ (\pm 0.06) + 0.131\ (\pm 0.017)\ C_m, R^2 = 0.934 \quad (2)$$

$$C_nMeImCl: A_{min}/nm^2 = 1.46\ (\pm 0.08) - 0.062\ (\pm 0.006)\ C_n, R^2 = 0.969 \quad (3)$$

Eqs. (1) and (2), and Table 1 show the following consequences of increasing the HG volume on the calculated values of the adsorption parameters of C_{16}RImX: (i) an increase in A_{min}, due to steric repulsions between the increasingly voluminous C_m groups [46]; (ii) a corollary to this increase in A_{min} is the presence of less surfactant molecules at the water/air interface which agrees with the decrease of Γ_{max} and increase in γ_{CMC}; (iii) the adsorption of a more hydrophobic HG is favored as shown by the increase in $|\Delta G^0_{ads}|$ and pC_{20}.

Regarding the effect of unsaturation in the HG, comparison of A_{min} of C_{16}EtImBr with C_{16}VnImBr, and C_{16}PrImBr with C_{16}AllmBr shows that

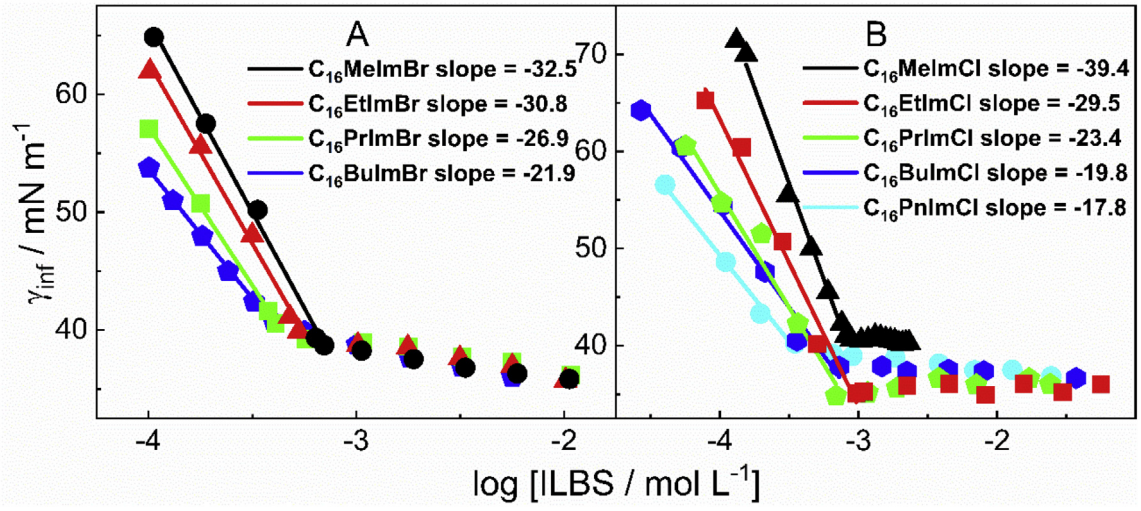

Fig. 3. Surface tension for t → infinite (γ_{inf}) as a function of logarithm of ILBS concentration, at 25 °C. Part A ($C_{16}C_m$ImBr) and Part B ($C_{16}C_m$ImCl). The straight lines before the cmc were used to calculate the minimum area per molecule at the water/air interface.

introduction of unsaturation is akin to removal of one methylene group. In this case, the double bond presumably increases the dipole-induced dipole intermolecular forces between the HGs and water molecules, leading to the HG approximation [12], hence to a smaller value of A_{min}. Comparison of γ_{cmc}, pC_{20}, and Γ_{max} of unsaturated and saturated HGs (Table 1) agrees with closer approximation between the molecules of the former surfactants. Comparison of the series $C_{16}C_m$ImX and C_nMeImCl shows the opposite effects of increasing the number of carbons in the HG and HC, respectively. The behavior in the C_nMeImCl series is explained by a concomitant closer packing of monomers at the micellar interface as a function of increasing the length of C_n [17,46–48].

The values of ΔG^0_{ads} can be divided into the contributions from the surfactant segments, namely, the *n*-hexadecylimidazolium ring + the counter-ion ($\Delta G^0_{ads,C16+Im+X}$) and C_m ($\Delta G^0_{ads,Cm}$) for the $C_{16}C_m$ImX series (Eq. (4)) and methylimidazolium ring + the counter-ion ($\Delta G^0_{ads,Me+Im+X}$), and C_n ($\Delta G^0_{ads,Cn}$) for the C_nMeImCl series (Eq. (5)).

$$\Delta G^0{}_{ads} = \Delta G^0{}_{ads,C16+Im+X} + \Delta G^0{}_{ads,Cm}\, C_m \tag{4}$$

$$\Delta G^0{}_{ads} = \Delta G^0{}_{ads,Me+Im+X} + \Delta G^0{}_{ads,Cn}\, C_n \tag{5}$$

Following these equations, the dependence of ΔG^0_{ads} on HG volume, and the length of the hydrophobic chain [17] is described by Eqs. (6), (7) and (8).

$$C_{16}C_m ImBr : \Delta G^0{}_{ads}/kJ\ mol^{-1} = -34.6\ (\pm 0.4) - 2.0\ (\pm 0.2)\ C_m, R^2 = 0.982 \tag{6}$$

$$C_{16}C_m ImCl : \Delta G^0{}_{ads}/kJ\ mol^{-1} = -33.1\ (\pm 0.9) - 2.5\ (\pm 0.3)\ C_m, R^2 = 0.955 \tag{7}$$

$$C_n MeImCl : \Delta G^0{}_{ads}/kJ\ mol^{-1} = -21.8\ (\pm 0.5) - 0.85\ (\pm 0.04)\ C_n, R^2 = 0.994 \tag{8}$$

The results of the regression analysis show that the change of ΔG^0_{ads} per CH_2 group in the HG and HC are 2.0–2.5 kJ mol^{-1} and 0.85 kJ mol^{-1}, respectively. This difference in ΔG^0_{ads} maybe related to changes in solvation entropy of the appropriate segment of both ILBSs series. Note that the methylene groups of C_nMeImCl are certainly less solvated (by water) than the C_m groups of $C_{16}C_m$ImX. Consequently, the expected order is $|\Delta S|_{CnMeImCl} > |\Delta S|_{C16CmImCl}$, in agreement with the calculated ΔG^0_{ads} of Table 1. Finally, the effects of the counter-ions on the adsorption parameters are small; they become more apparent in the micellar aggregates, *vide infra.*

3.3. Micelle formation

Values of the cmcs were calculated from conductivity and surface tension data; in both cases from the intercept of two straight lines were calculated from the plotted data. Surface tension data were analyzed in Section 3.2.

As expected, the specific conductance increases fast until the cmc, and then less after micelle formation, because conductivity of the latter species (a macroion) [49] is less than the free, *i.e.*, dissociated surfactant monomers. Fig. 4 shows typical conductivity data for both series, the calculated values of cmc and other micellar parameters are listed in Table 2. The calculation methods of the micellization parameters are discussed at Section 3.2. of SM. Carpena's method, see Eq. SM5, is especially adequate for the analysis of cases where the change in the slopes before and after the cmc is not sharp. This gradual change in conductivity may be associated with the formation of premicellar aggregates and is more pronounced for ILBS with $C_m = 4$ and 5, *vide infra.*

The cmc values calculated from the data of both techniques are in excellent agreement, considering that these techniques are sensitive to different aspects of the micellization process, as discussed in detail elsewhere [51]. In most cases, close to room temperature, the driving force for micelle formation is entropic. The reason is that the transfer of the HC from water into the micelle, and the HG into (less polar) interfacial water is associated with release of the highly-ordered water molecules around the hydrocarbon chains of both surfactant segments. Further entropy gain on micellization is due to the increase in the degrees of freedom of the HC inside the micelle, relative to bulk water [52]. Therefore, it is expected that values of the cmc decrease as a function of increasing both C_n and C_m, as shown in Table 2. Stauff-Klevens rule [53] (Eq. (9)) predicts a linear relationship between the log cmc and C_n:

$$log\ cmc = A - B\ C_n \tag{9}$$

where A is a constant that depends on the structure of the surfactant monomer, and B reflects the effect of each additional CH_2 on cmc. We applied this equation to C_m and C_n; the results of the regression analysis are shown in Eqs. (10)–(13), and plotted graphically in Fig. SM17.

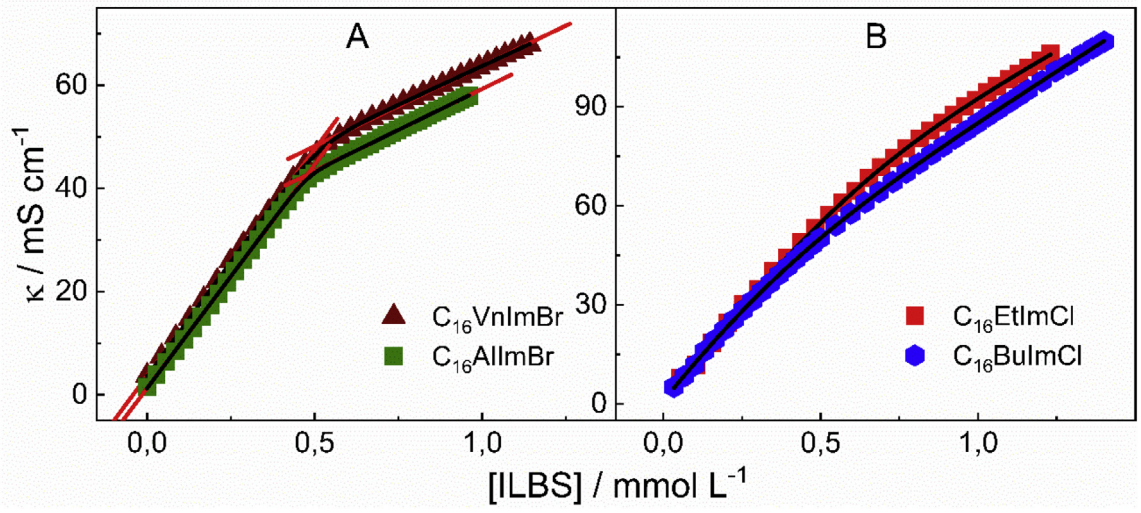

Fig. 4. Specific conductance (κ) as a function of surfactant concentration. The red straight lines are drawn to determine the cmc values visually and the black curve represents the regression by the Carpena equation. Part A and Part B are representative plots of bromide and chloride ILBSs, respectively.

Table 2
Values of micellization parameters, including cmc, N_{agg} and α_{mic} determined by experimental and theoretical techniques for ILBSs, at 25 °C.

ILBS	cmc (mmol L^{-1})		N_{agg} [a]	α_{mic} (Evans) [b]	α_{mic} (Frahm) [c]	ΔG^0_{mic} [d] (kJ mol^{-1})
	Surface tension	Conductivity				
Bromide ILBSs						
C_{16}MeImBr	0.71	0.65	64[e]	0.133	0.283	−52.59
C_{16}EtImBr	0.55	0.52	60[f]	0.150	0.344	−53.09
C_{16}PrImBr	0.44	0.41	52	0.178	0.440	−53.41
C_{16}BuImBr	0.40	0.30	45	0.198	0.498	−54.30
C_{16}VnImBr	0.60	0.52	54[f]	0.154	0.338	−53.01
C_{16}AllmBr	0.51	0.48	47	0.168	0.366	−52.98
Chloride ILBSs						
C_{16}MeImCl	0.87	0.91	97[g]	0.220	–	−48.63
C_{16}EtImCl	0.88	0.58	83	0.274	–	−49.10
C_{16}PrImCl	0.71	0.46	71	0.298	–	−49.37
C_{16}BuImCl	0.50	0.51	61	0.278	–	−49.52
C_{16}PnImCl	0.35	0.39	53	0.304	–	−49.90

[a] Values of N_{agg} were obtained by theoretical calculation, see Section 3.2. in SM.
[b] Calculated from Eq. SM7.
[c] Calculated from Eq. SM8.
[d] Values of Gibb's free energy of micellization (ΔG^0_{mic}) calculated with α_{mic} from Evans method.
[e] Value of reference [35], calculated from steady state fluorescence measurements.
[f] Values of reference [12], calculated from steady state fluorescence measurements.
[g] Value of reference [50], calculated from static light scattering measurements.

$$C_{16}C_mImBr : log\left(cmc/mol\,L^{-1}\right) = -3.075\ (\pm 0.008) - 0.097\ (\pm 0.003)\ C_m, R^2 = 0.997 \quad (10)$$

$$C_{16}C_mImCl : log\left(cmc/mol\,L^{-1}\right) = -2.953\ (\pm 0.019) - 0.092\ (\pm 0.006)\ C_m, R^2 = 0.985 \quad (11)$$

$$C_{16}(C_m)_3NBr : log\left(cmc/mol\,L^{-1}\right) = -2.75\ (\pm 0.17) - 0.21\ (\pm 0.06)\ C_m, R^2 = 0.851 \quad (12)$$

$$C_nMeImBr : log\left(cmc/mol\,L^{-1}\right) = 1.79\ (\pm 0.04) - 0.304\ (\pm 0.003)\ C_n, R^2 = 0.999 \quad (13)$$

It is interesting that the Stauff-Klevens rule is also applicable for the HG, resulting in excellent linear correlation between the log cmc and (C_m). This type of correlation was also deducted for the conventional surfactant series $C_{16}(C_m)_3NBr$ (cmc data from Ref. [54]), Eq. (12). The lower value of the constant (A) for the $C_{16}C_m$ImBr series shows that the structure of ILBSs monomer (not considering the side chain) favors the formation of micelles at smaller concentrations than the conventional surfactant series. To compare the values of (B) for both series, it is important to consider that for the $C_{16}(C_m)_3NBr$ series there is an increase of 3 CH_2 groups for each one of the $C_{16}C_m$ImBr series. Therefore, it is necessary to divide the values of (B) of Eq. (12) by 3. We found that |B; $C_{16}C_m$ImBr| > |B; $C_{16}(C_m)_3NBr/3$|, the former surfactant series is more surface active.

The fact that the slope per CH_2 in the HC series, Eq. (13), is *ca.* 3 times larger than in the HG series, Eq. (10), is not surprising because on micellization there is more dehydration of most of the CH_2 groups in HC (whose micelle interior is oil-like) that any CH_2 in the HG; the latter is transferred from bulk- to less polar water, *vide infra*. The (slight) difference in polarity between bulk- and interfacial water also explains the little dependence of ΔG^0_{mic} on the presence of unsaturation in the HG. On the other hand, micellization of $C_{16}C_m$ImBr is more favorable than the corresponding $C_{16}C_m$ImCl because the formation of micelles is more spontaneous for bromides due to the larger ion size and polarizability of Br^-, which decreases the repulsion between the cationic head-ions in the formed micelle, [55] hence lowers the cmc values.

As shown in Table 2, the values of α_{mic} increase as a function of increasing HG volume. The increased dissociation of the counter-ion is induced by an increased steric hindrance around the imidazolium ring which prevents the approach of the halide ion to the cation at the micellar interface [56]. Based on Eq. SM6, this increase in α_{mic} decreases the corresponding value of ΔG^0_{mic}, as shown in Fig. 5. The linear regressions of the lines in Fig. 5 are shown in Eqs. (14), (15) and (16), and highlights the fact that the contribution of HG volume increase is much smaller (10% for the chloride ILBSs) relative to the same increase in the HC.

$$C_{16}C_mImBr : \Delta G^0{}_{mic}/kJ\ mol^{-1} = -52.0\ (\pm 0.2) - 0.54\ (\pm 0.08)\ C_m, R^2 = 0.936 \quad (14)$$

$$C_{16}C_mImCl : \Delta G^0{}_{mic}/kJ\ mol^{-1} = -48.42\ (\pm 0.10) - 0.30\ (\pm 0.03)\ C_m, R^2 = 0.971 \quad (15)$$

$$C_nMeImCl : \Delta G^0{}_{mic}/kJ\ mol^{-1} = 2.1\ (\pm 1.0) - 3.16\ (\pm 0.08)\ C_n, R^2 = 0.936 \quad (16)$$

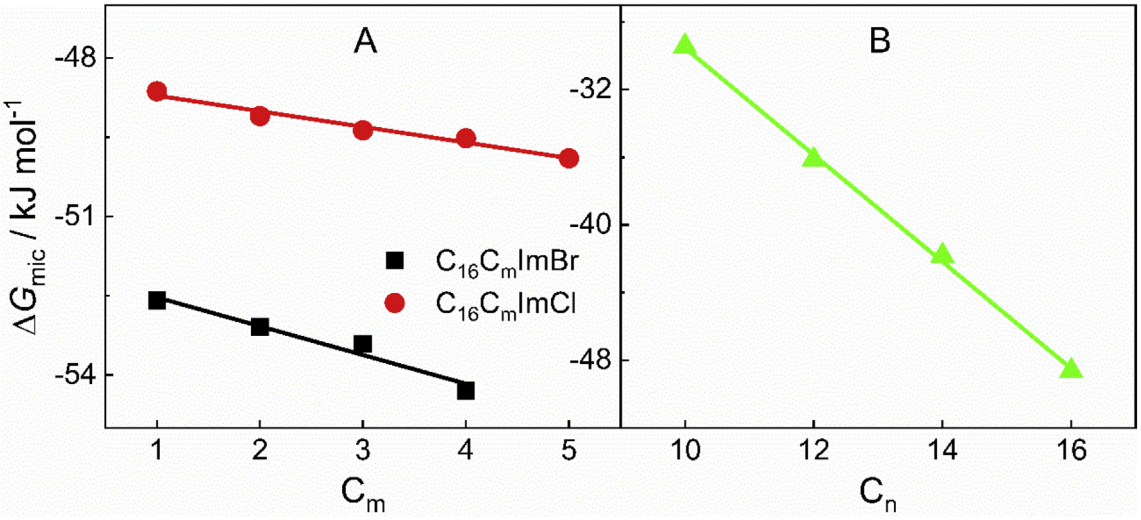

Fig. 5. Dependence of Gibb's free energy of micellization (ΔG^0_{mic}) on the number of carbon atom (C_m or C_n), at 25 °C. Part A ($C_{16}C_m$ImX) and Part B (C_nMeImCl) [57].

3.4. Microscopic polarity and concentration of the interfacial water

Fluorescence measurements with pyrene were performed for $C_{16}C_m$ImX to calculate the microscopic polarity, hence the concentration of interfacial water ($[H_2O]_{int}$). Monomeric pyrene exhibits five vibronic peaks in the region between 375 and 410 nm due to π-π* transitions. The ratio of fluorescence intensities of the first and third vibronic peaks (I_1/I_3) is sensitive to the microscopic polarity experienced by the pyrene molecules. Since the third peak shows higher fluorescence intensity compared to the first one in a hydrophobic environment, an increase in hydrophobicity is indicated by a relatively lower value of the I_1/I_3 ratio [58]. An example of pyrene fluorescent graph is shown at Fig. SM18. ^{1}H NMR data for sodium dodecylbenzene sulfonate indicated that the *average* solubilization site of the pyrene molecule is the interfacial region, close to the surfactant aromatic head-group [59]. Additionally, ^{1}H NMR and fluorescence studies on ILBSs with aromatic counter-ions [60,61], and interactions of cationic ILBSs with sodium dodecylbenzene sulfonate [62] clearly showed the preference of the aromatic rings to associate with the imidazolium cation. Consequently, we can safely assume that pyrene will be similarly solubilized in the interfacial region, close to the heterocyclic ring.

The results of microscopic polarity (I_1/I_3) (displayed at Table SM2) show that the interfacial water of the studied ILBSs solutions ($I_1/I_3 \approx 1.31$) is less polar than bulk water ($I_1/I_3 = 1.84$ [37]), the interfacial water concentration decreases linearly as a function of increasing the volume of HG, from 41.6 mol L^{-1} for C_{16}MeImCl to 38.2 mol L^{-1} for C_{16}PnImCl, and there is only a slight dependence on the counter-ion. It is interesting that this concentration range 40 ± 2 mol L^{-1} is similar to that calculated for conventional cationic surfactants using a solvatochromic probe [38], and that inferred from a distinct approach, namely, reaction of micelle incorporated diazonium ion with water, the so-called ion-trapping technique [63]. This agreement is satisfactory and shows that pyrene is an appropriate probe for calculating $[H_2O]_{int}$.

3.5. Solubilization of lipophilic dye and drug

The solubilization of Sudan IV and nitrendipine in aqueous solutions of the series of ILBSs was investigated. Measurements were not done for C_{16}BuImBr because the surfactant precipitated during dissolution of both solubilizates. The molar extinction coefficients (ε_0) for both molecules in aqueous media are known, 7.5×10^{-4} mol^{-1} cm^{-1} for Sudan IV and 3.2×10^{-3} mol^{-1} cm^{-1} for nitrendipine [64,65], therefore the concentration of the dissolved solute can be readily calculated from the Beer's law plot, assuming the same values of ε_0.

The molar solubilization power (*SP*) of a surfactant is defined as moles of solubilized molecule per mole of micellized surfactant. If the micellar aggregation number is not influenced by the solubilization of the dye or drug, the solubilization capacity (Σ), which is the average number of molecules solubilized in each micelle is defined by Eq. (17) [66].

$$\Sigma = N_{agg}\, x\, SP = N_{agg}\, x\, \frac{S_{total} - S_{water}}{[ILBS] - CMC} \quad (17)$$

where S_{total} and S_{water} refer to the solubility of the molecule in presence, and absence of the surfactant, respectively [66].

Surprisingly, the values of *SP* of Sudan IV and nitrendipine in micellar $C_{16}C_m$ImX *decreased* linearly as a function of increasing C_m, as shown in Table 3 and Fig. SM19. In addition to solute-micelle hydrophobic interactions, other factors should be considered, namely the micelle size, and steric hindrance. As shown in Table 2, N_{agg} for these ILBS decreases linearly with the increase of C_m; consequently, the micelles become smaller, leading to a decrease in the number of solute molecules that can be accommodated. It is also plausible that this effect is coupled to increased steric hindrance to solute penetration in micellar pseudo-phase.

Table 3 shows much higher solubilization capacity for nitrendipine than for Sudan IV by both $C_{16}C_m$ImX. Whether the drug induces micelle morphology change (*e.g.*, from spherical micelles → vesicles), akin to other drugs (*e.g.*, cholesterol and diclofenac sodium [15,67]) is an open question. The difference between solubilization power of bromides and chlorides ILBSs can be disregarded for Sudan IV, as it is <5%. For nitrendipine the corresponding difference is >25%, clearly showing that the counter-ion is important. This may be taken as another indication for the above-mentioned, drug-induced morphology change, a subject that we intend to investigate. Finally, it is worth mentioning that the solubilization power of Sudan IV by the present ILBSs is 2 to 3 times higher than CTAB [66], a conventional cationic surfactant. To the best of our knowledge, no other study has been done with the dissolution of nitrendipine in micellar ILBSs.

Table 3
Solubilization power, *SP*, and solubilization capacity, $\sum$, of ILBSs for Sudan IV and nitrendipine.

ILBS	Sudan IV		Nitrendipine	
	SP	$\sum$ (molecule micelle^{-1})	*SP*	$\sum$ (molecule micelle^{-1})
Bromide ILBSs				
C_{16}MeImBr	0.0175	1.1	1.09	70
C_{16}EtImBr	0.0168	1.0	0.968	58
C_{16}PrImBr	0.0161	0.8	0.743	39
Chloride ILBSs				
C_{16}MeImCl	0.0166	1.6	1.50	146
C_{16}EtImCl	0.0160	1.3	1.32	110
C_{16}PrImCl	0.0154	1.1	1.16	82
C_{16}BuImCl	0.0149	0.9	0.938	57
C_{16}PnImCl	0.0146	0.8	0.727	38

4. Conclusions

The synthetic routes employed (microwave-assisted; one is solventless) produced surface-active pure surfactants. Information about adsorption, micellization and micelle interfacial water concentration of C_{16}RImX (X = Br and Cl) in aqueous solutions were obtained from surface tension and conductivity data, and fluorescence of micelle-solubilized pyrene, respectively. Values of γ employed in the calculations were those after attaining surfactant adsorption equilibrium at the water/air interface. Use of Carpena's method for the calculation of the cmc was especially helpful for $C_{16}C_m$ImX, C_m = 4 and 5, where formation of premicellar aggregates probably occurs. Values of cmc calculated from both techniques were in excellent agreement.

The structural modification of ILBSs caused by introduction of methylene (CH_2) in the HG causes a decrease in polarity, with concomitant increase in surface tension reduction in efficiency (pC_{20}), A_{min}, and α_{mic} and a decrease in cmc, ΔG^0_{mic}, N_{agg}, and $[H_2O]_{int}$. The presence of unsaturation in the HG proved to be as relevant as the variation in the number of CH_2, being comparable to the removal of one CH_2 due to the less hydrophobic character of the double bond. The changes caused by increasing the HG volume are less pronounced than those due to increasing the length of HC. Values of $[H_2O]_{int}$ (40 ± 2 mol L^{-1}), obtained by fluorescence of micelle-solubilized pyrene, are similar to those calculated by different approaches, based on the use of solvatochromic probes and the reaction of micelle-incorporated diazonium ion with water. Solubilization of Sudan IV and nitrendipine decreased as a function of increasing the HG volume, probably reflecting steric hindrance to the penetration of the solubilizate in smaller micelles. Comparing the ILBSs of this study with conventional surfactants with the same hydrophobic tail showed that the former class has superior surface activity, lower cmc values, and are more effective in hydrophobic dye (Sudan IV) dissolution [10,11,66].

Author statement

Nicolas Keppeler: Data curation; formal analysis; methodology, writing. Paula D. Galgano: data curation, formal analysis, methodology. Soraya S. Santos: data curation, methodology. Naved I Malek: formal analysis, writing. Omar A. El Seoud: conceptualization, writing, formal analysis, funding aquisition.

Declaration of Competing Interest

The authors declare that they have no known competing financial interests or personal relationships that could have appeared to influence the work reported in this paper.

Acknowledgments

We thank São Paulo State Research Foundation (FAPESP) for financial support (grant 2014/22136-4); the National Council for Scientific and Technological Research (CNPq) for a pre-doctoral fellowship to N. Keppeler, and a research productivity fellowship to O. A. El Seoud (grant 306108/2019-4). NIM acknowledge the financial assistance of UGC-DAE for the Collaborative Research Scheme (UDCSR/MUM/AO/CRS-M-276/2017). We are indebted to Prof. Iolanda M. Cuccovia for making the fluorescence spectrophotometer available to us, and Dr. Paulo A.R. Pires for his help with theoretical calculations.

Appendix A. Supplementary material

Supplementary data to this article can be found online at https://doi.org/10.1016/j.molliq.2021.115478.

References

[1] N.V. Plechkova, K.R. Seddon, Applications of ionic liquids in the chemical industry, Chem. Soc. Rev. 37 (2008) 123–150, https://doi.org/10.1039/b006677j.
[2] I.M. Marrucho, L.C. Branco, L.P.N. Rebelo, Ionic liquids in pharmaceutical applications, Ann. Rev. Chem. Biomol. Eng. 5 (2014) 527–546, https://doi.org/10.1146/annurev-chembioeng-060713-040024.
[3] U. König, B. Sessler, Ionic liquids in plating industry: opportunities and challenges, Trans. Inst. Met. Finish. 86 (2008) 183–188, https://doi.org/10.1179/174591908X327509.
[4] P.D. Galgano, O.A. El Seoud, Ionic liquid-based surfactants: Synthesis, molecular structure, micellar properties and applications, in: B.K. Paul, S.P. Moulik (Eds.), Ionic Liquid-Based Surfactant Science: Formulation, Characterization, and Applications, 1st edJohn Wiley & Sons Inc 2015, pp. 63–99, https://doi.org/10.1002/9781118854501.ch4.
[5] N. Adawiyah, M. Moniruzzaman, S. Hawatulaila, M. Goto, Ionic liquids as a potential tool for drug delivery systems, MedChemComm. 7 (2016) 1881–1897, https://doi.org/10.1039/c6md00358c.
[6] A.A. Shamsuri, Ionic liquids: preparations and limitations, MAKARA Sci. Series. 14 (2011) 101–106, https://doi.org/10.7454/mss.v14i2.677.
[7] M. Moniruzzaman, K. Nakashima, N. Kamiya, M. Goto, Recent advances of enzymatic reactions in ionic liquids, Biochem. Eng. J. 48 (2010) 295–314, https://doi.org/10.1016/j.bej.2009.10.002.
[8] M. Kaur, H. Kaur, M. Singh, G. Singh, T.S. Kang, Biamphiphilic ionic liquid based aqueous microemulsions as an efficient catalytic medium for cytochrome c, Phys. Chem. Chem. Phys. 19 (2021)https://doi.org/10.1039/d0cp04513f.
[9] M. Kaur, G. Singh, A. Kaur, P.K. Sharma, T.S. Kang, Thermally stable ionic liquid-based microemulsions for high-temperature stabilization of lysozyme at nanointerfaces, Langmuir. 35 (2019) 4085–4093, https://doi.org/10.1021/acs.langmuir.9b00106.
[10] X.J. Yang, P. Zhang, W. Lv, T. Zhou, P. Li, M. Zhao, Aggregation behavior of Imidazolium-based amino acid ionic liquid surfactants in aqueous solution: the effect of amino acid Counterions, J. Surfactant Deterg. 22 (2019) 515–523, https://doi.org/10.1002/jsde.12270.
[11] B. Dong, N. Li, L. Zheng, L. Yu, T. Inoue, Surface adsorption and micelle formation of surface active ionic liquids in aqueous solution, Langmuir. 23 (2007) 4178–4182, https://doi.org/10.1021/la0633029.
[12] N.I. Malek, Z.S. Vaid, U.U. More, O.A. El Seoud, Ionic-liquid-based surfactants with unsaturated head group: synthesis and micellar properties of 1-(n-alkyl)-3-vinylimidazolium bromides, Colloid Polym. Sci. 293 (2015) 3213–3224, https://doi.org/10.1007/s00396-015-3746-x.
[13] N. Azum, A.Z. Naqvi, M. Akram, Kmaabir-ud-Din, Studies of mixed micelle formation between cationic gemini and cationic conventional surfactants, J. Colloid Interface Sci. 328 (2008) 429–435, https://doi.org/10.1016/j.jcis.2008.09.034.
[14] Z.S. Vaid, S.M. Rajput, A. Shah, Y. Kadam, A. Kumar, O.A. El Seoud, J.P. Mata, N.I. Malek, Salt-induced microstructural transitions in aqueous dispersions of ionic-liquids-based surfactants, ChemistrySelect. 3 (2018) 4851–4858, https://doi.org/10.1002/slct.201800041.
[15] Z.S. Vaid, S.M. Rajput, M. Kuddushi, A. Kumar, O.A. El Seoud, N.I. Malek, Synergistic interaction between cholesterol and functionalized ionic liquid based surfactant leading to the morphological transition, ChemistrySelect. 3 (2018) 1300–1308, https://doi.org/10.1002/slct.201702561.
[16] I. Pacheco-fernández, V. Pino, J.H. Ayala, A.M. Afonso, Ionic liquid-based surfactants: A step forward, in: A. Eftekhari (Ed.), Ionic Liquid Devices, Royal Society of Chemistry, Croydon 2017, pp. 53–72.
[17] O.A. El Seoud, P.A.R. Pires, T. Abdel-Moghny, E.L. Bastos, Synthesis and micellar properties of surface-active ionic liquids: 1-Alkyl-3-methylimidazolium chlorides, J. Colloid Interface Sci. 313 (2007) 296–304, https://doi.org/10.1016/j.jcis.2007.04.028.
[18] P.C. Hiemenz, R. Rajagopalan, Principles of Colloid and Surface Chemistry, 3rd ed. Marcel Dekker, New York, 1997.
[19] M. Yasuda, K. Ikeda, K. Esumi, K. Meguro, Effect of head group size on aqueous properties of α,ω-type surfactant, Langmuir. 6 (1990) 949–953, https://doi.org/10.1021/la00095a011.
[20] A. Di Michele, L. Brinchi, P. Di Profio, R. Germani, G. Savelli, G. Onori, Effect of head group size, temperature and counterion specificity on cationic micelles, J. Colloid Interface Sci. 358 (2011) 160–166, https://doi.org/10.1016/j.jcis.2010.12.028.
[21] H. Xing, P. Yan, K.S. Zhao, J.X. Xiao, Effect of headgroup size on the thermodynamic properties of micellization of dodecyltrialkylammonium bromides, J. Chem. Eng. Data 56 (2011) 865–873, https://doi.org/10.1021/je100598x.
[22] E. Akpinar, E. Guner, O. Demir-Ordu, A.M.F. Neto, Effect of head-group size of some tetradecylalkylammonium bromide surfactants on obtaining the lyotropic biaxial nematic phase, Eur. Phys. J. E. 42 (2019) 1–8, https://doi.org/10.1140/epje/i2019-11806-y.
[23] A. Pal, S. Yadav, Effect of anionic polyelectrolyte sodium carboxymethylcellulose on the aggregation behavior of surface active ionic liquids in aqueous solution, J. Mol. Liq. 241 (2017) 584–594, https://doi.org/10.1016/j.molliq.2017.06.063.
[24] L. Qin, X.H. Wang, Surface adsorption and thermodynamic properties of mixed system of ionic liquid surfactants with cetyltrimethyl ammonium bromide, RSC Adv. 7 (2017) 51426–51435, https://doi.org/10.1039/c7ra08915e.
[25] G.Y. Wang, Y.Y. Wang, X.H. Wang, Aggregation behaviors of mixed systems for imidazole based ionic liquid surfactant and Triton X-100, J. Mol. Liq. 232 (2017) 55–61, https://doi.org/10.1016/j.molliq.2017.02.044.
[26] Q.Q. Baltazar, J. Chandawalla, K. Sawyer, J.L. Anderson, Interfacial and micellar properties of imidazolium-based monocationic and dicationic ionic liquids, Colloids Surf. A Physicochem. Eng. Asp. 302 (2007) 150–156, https://doi.org/10.1016/j.colsurfa.2007.02.012.
[27] C. Jungnickel, J. Łuczak, J. Ranke, J.F. Fernández, A. Müller, J. Thöming, Micelle formation of imidazolium ionic liquids in aqueous solution, Colloids Surf. A Physicochem. Eng. Asp. 316 (2008) 278–284, https://doi.org/10.1016/j.colsurfa.2007.09.020.
[28] S. Thomaier, W. Kunz, Aggregates in mixtures of ionic liquids, J. Mol. Liq. 130 (2007) 104–107, https://doi.org/10.1016/j.molliq.2006.04.013.
[29] N.V. Sastry, N.M. Vaghela, V.K. Aswal, Effect of alkyl chain length and head group on surface active and aggregation behavior of ionic liquids in water, Fluid Phase Equilib. 327 (2012) 22–29, https://doi.org/10.1016/j.fluid.2012.04.013.
[30] S. Chabba, R. Vashishat, T.S. Kang, R.K. Mahajan, Self – aggregation behavior of Dialkyl Imidazolium based ionic liquids in aqueous medium : effect of alkyl chain length, ChemistrySelect. 1 (2016) 2458–2470, https://doi.org/10.1002/slct.201600301.
[31] R. Trouve, G. Nahas, Nitrendipine: an antidote to cardiac and lethal toxicity of cocaine, Proc. Soc. Exp. Biol. Med. 183 (1986) 392–397, https://doi.org/10.3181/00379727-183-3-RC1.
[32] A.J.M. Valente, O. Söderman, The formation of host-guest complexes between surfactants and cyclodextrins, Adv. Colloid Interf. Sci. 205 (2014) 156–176, https://doi.org/10.1016/j.cis.2013.08.001.
[33] W.L.F. Armarego, Purification of Laboratory Chemicals, 8th ed Elsevier, 2008.
[34] G.F. Longman, The analysis of detergents, Talanta. 22 (1975) 621–636.
[35] H.-L. Su, M.-S. Lan, Y.-Z. Hsieh, Using the cationic surfactants N-cetyl-N-methylpyrrolidinium bromide and 1-cetyl-3-methylimidazolium bromide for sweeping–micellar electrokinetic chromatography, 2017https://doi.org/10.1016/j.chroma.2009.05.001.
[36] P.D. Galgano, O.A. El Seoud, Micellar properties of surface active ionic liquids: a comparison of 1-hexadecyl-3-methylimidazolium chloride with structurally related cationic surfactants, J. Colloid Interface Sci. 345 (2010) 1–11, https://doi.org/10.1016/j.jcis.2010.01.078.
[37] Y. Kusumoto, Y. Takeshita, J. Kurawaki, I. Satake, Preferential solvation studied by the fluorescence spectrum of pyrene in water-alcohol binary mixtures, Chem. Lett. (1997) 349–350.
[38] E.B. Tada, L.P. Novaki, O.A. El Seoud, Solvatochromism in cationic micellar solutions: effects of the molecular structures of the solvatochromic probe and the surfactant headgroup, Langmuir. 17 (2001) 652–658, https://doi.org/10.1021/la001135l.
[39] L. Ye, F. Chen, J. Liu, A. Gao, G. Kircher, W. Liu, M. Kappl, S. Wegner, H.J. Butt, W. Steffen, Responsive Ionogel surface with renewable antibiofouling properties, Macromol. Rapid Commun. 40 (2019) 1–6, https://doi.org/10.1002/marc.201900395.
[40] J. Shen, W. He, T. Wang, Multifunctional amphiphilic ionic liquid pathway to create water-based magnetic fluids and magnetically-driven mesoporous silica, RSC Adv. 9 (2019) 3504–3513, https://doi.org/10.1039/c8ra10065a.
[41] H. Matsuki, M. Yamanaka, Y. Yamashita, S. Kaneshina, Adsorption-equilibrium surface tension of surfactant solutions; examination by the drop volume method, Bull. Chem. Soc. Jpn. 79 (2006) 1704–1710, https://doi.org/10.1246/bcsj.79.1704.

[42] E.E. Dreger, G. Klein, G. Miles, L. Shedlovsky, J. Ross, Sodium alcohol sulfates.properties involving surface activity, Ind. Eng. Chem. 36 (1944) 610–617, https://doi.org/10.1021/ie50415a004.
[43] D.J. Lee, Enthalpy-entropy compensation in ionic micelle formation, Colloid Polym. Sci. 273 (1995) 539–543, https://doi.org/10.1007/BF00658683.
[44] K. Lunkenheimer, R. Miller, A criterion for judging the purity of adsorbed surfactant layers, J. Colloid Interface Sci. 120 (1987) 176–183, https://doi.org/10.1016/0021-9797(87)90337-7.
[45] K. Lunkenheimer, H.J. Pergande, H. Krüger, Apparatus for programmed high-performance purification of surfactant solutions, Rev. Sci. Instrum. 58 (1987) 2313–2316, https://doi.org/10.1063/1.1139343.
[46] M.J. Rosen, L. Liu, Surface activity and premicellar aggregation of some novel diquaternary gemini surfactants, JAOCS, J. Am. Oil Chem. Soc. 73 (1996) 885–890, https://doi.org/10.1007/BF02517990.
[47] R. Hadgiivanova, H. Diamant, Premicellar aggregation of amphiphilic molecules, J. Phys. Chem. B 111 (2007) 8854–8859, https://doi.org/10.1021/jp070038z.
[48] P. Lianos, R. Zana, Micelles of tetradecyltrialkylammonium bromides with fluorescent probes, J. Colloid Interface Sci. 88 (1982) 594–598, https://doi.org/10.1016/0021-9797(82)90289-2.
[49] P.C. Schulz, M.E. Hernandez-Vargas, J.E. Puig, Do micelles contribute to the total conductivity of ionic micellar systems? Lat. Am. Appl. Res. 25 (1995) 153–159.
[50] P.D. Galgano, O.A. El Seoud, Surface active ionic liquids: study of the micellar properties of 1-(1-alkyl)-3-methylimidazolium chlorides and comparison with structurally related surfactants, J. Colloid Interface Sci. 361 (2011) 186–194, https://doi.org/10.1016/j.jcis.2011.04.108.
[51] P. Mukerjee, The nature of the association equilibria and hydrophobic bonding in aqueous solutions of association colloids, Adv. Colloid Interf. Sci. 1 (1967) 242–275, https://doi.org/10.1016/0001-8686(67)80005-8.
[52] M.J. Rosen, Surface and Interfacial Phenomena, 2nd ed. Wiley-VCH Verlag GmbH & Co, KGaA, New York, 1989.
[53] H.B. Klevens, Structure and aggregation in dilate solution of surface active agents, J. Am. Oil Chem. Soc. 30 (1953) 74–80, https://doi.org/10.1007/BF02635002.
[54] M.A. Rodríguez, M. Muñoz, M. del Graciani, M.S. Fernández Pachón, M.L. Moyá, Effects of head group size on micellization of cetyltrialkylammonium bromide surfactants in water-ethylene glycol mixtures, Colloids Surf. A Physicochem. Eng. Asp. 298 (2007) 177–185, https://doi.org/10.1016/j.colsurfa.2006.10.062.
[55] S. Manet, Y. Karpichev, D. Bassani, R. Kiagus-Ahmad, R. Oda, Counteranion effect on micellization of cationic gemini surfactants 14-2-14: Hofmeister and other counterions, Langmuir. 26 (2010) 10645–10656, https://doi.org/10.1021/la1008768.
[56] R. Zana, Ionization of cationic micelles: effect of the detergent structure, J. Colloid Interface Sci. 78 (1980) 330–337, https://doi.org/10.1016/0021-9797(80)90571-8.
[57] P.D. Galgano, Líquidos Iônicos Tensoativos: Correlação entre Estrutura Molecular e Propriedades Micelares de Cloretos de 1,3-dialquilimidazólio, 2012.
[58] M. Akram, F. Ansari, Kabir-ud-Din, Biophysical investigation of the interaction between cationic biodegradable Cm-E2O-Cm gemini surfactants and porcine serum albumin (PSA), Spectrochim. Acta - Part A. 206 (2019) 520–528, https://doi.org/10.1016/j.saa.2018.08.043.
[59] X. Yang, G. Lu, B. She, X. Liang, R. Yin, C. Guo, X. Yi, Z. Dang, Cosolubilization of 4,4′-dibromodiphenyl ether, naphthalene and pyrene mixtures in various surfactant micelles, Chem. Eng. J. 260 (2015) 74–82, https://doi.org/10.1016/j.cej.2014.08.101.
[60] O. Singh, P. Singla, V.K. Aswal, R.K. Mahajan, Impact of aromatic counter-ions charge delocalization on the Micellization behavior of surface-active ionic liquids, Langmuir. 35 (2019) 14586–14595, https://doi.org/10.1021/acs.langmuir.9b02695.
[61] G. Singh, G. Singh, T.S. Kang, Micellization behavior of surface active ionic liquids having aromatic counterions in aqueous media, J. Phys. Chem. B 120 (2016) 1092–1105, https://doi.org/10.1021/acs.jpcb.5b09688.
[62] S. Chabba, S. Kumar, V.K. Aswal, T.S. Kang, R.K. Mahajan, Interfacial and aggregation behavior of aqueous mixtures of imidazolium based surface active ionic liquids and anionic surfactant sodium dodecylbenzenesulfonate, Colloids Surf. A Physicochem. Eng. Asp. 472 (2015) 9–20, https://doi.org/10.1016/j.colsurfa.2015.02.032.
[63] V. Soldi, J. Keiper, L.S. Romsted, I.M. Cuccovia, H. Chaimovich, Arenediazonium salts: New probes of the interfacial compositions of association colloids. 6. Relationships between interfacial counterion and water concentrations and surfactant headgroup size, sphere-to-rod transitions, and chemical reactivity in cationi, Langmuir. 16 (2000) 59–71, https://doi.org/10.1021/la990336q.
[64] S. Kumar, H.N. Singh, Competitive solubilization of Sudan IV and anthracene in micellar systems, Colloids Surf. A Physicochem. Eng. Asp. 69 (1992) 1–4, https://doi.org/10.1016/0166-6622(92)80231-P.
[65] S. Onoue, N. Igarashi, Y. Yamauchi, N. Murase, Y. Zhou, T. Kojima, S. Yamada, Y. Tsuda, In vitro phototoxicity of dihydropyridine derivatives: a photochemical and photobiological study, Eur. J. Pharm. Sci. 33 (2008) 262–270, https://doi.org/10.1016/j.ejps.2007.12.004.
[66] A.R. Tehrani-Bagha, K. Holmberg, Solubilization of hydrophobic dyes in surfactant solutions, Materials. 6 (2013) 580–608, https://doi.org/10.3390/ma6020580.
[67] Z.S. Vaid, A. Kumar, O.A. El Seoud, N.I. Malek, Drug induced micelle-to-vesicle transition in aqueous solutions of cationic surfactants, RSC Adv. 7 (2017) 3861–3869, https://doi.org/10.1039/c6ra25577a.